Proc. Natl. Acad. Sci. USA
Vol. 93, pp. 6851–6856, July 1996
Chemistry

Probing the oligomeric structure of an enzyme by electrospray ionization time-of-flight mass spectrometry

MICHAEL C. FITZGERALD*, IGOR CHERNUSHEVICH†‡, KENNETH G. STANDING†, CHRISTIAN P. WHITMAN§, AND STEPHEN B. H. KENT*

*The Scripps Research Institute, La Jolla, CA 92037; †Department of Physics, University of Manitoba, Winnipeg, MB Canada R3T 2N2; and §Medicinal Chemistry Division, College of Pharmacy, University of Texas, Austin, TX 78712

Communicated by Harry B. Gray, California Institute of Technology, Pasadena, CA, March 18, 1996 (received for review January 19, 1996)

ABSTRACT **Electrospray ionization time-of-flight (ESI–TOF) mass spectrometry was used to study the quaternary structure of 4-oxalocrotonate tautomerase (EC 5.3.2; 4OT), and four analogues prepared by total chemical synthesis. Wild-type 4OT is a hexamer of 62 amino acid subunits and contains no cysteine residues. The analogues were: (*des*Pro[1])4OT, a truncated construct in which Pro[1] was deleted; (Cpc[1])4OT in which Pro[1] was replaced with cyclopentane carboxylate; a derivative [Met(O)[45]]4OT in which Met[45] was oxidized to the sulfoxide; and an analogue (Nle[45])4OT in which Met[45] was replaced with norleucine. ESI of (Nle[45])4OT, (Cpc[1])4OT, and 4OT from solution conditions under which the native enzyme was fully active (5 mM ammonium bicarbonate buffer, pH 7.5) gave the intact hexamer as the major species detected by TOF mass spectrometry. In contrast, analysis of [Met(O)[45]]4OT and (*des*Pro[1])4OT under similar conditions yielded predominantly monomer ions. The ESI–TOF measurements were consistent with structural data obtained from circular dichroism spectroscopy. In the context of kinetic data collected for 4OT and these analogues, ESI–TOF mass spectrometry also provided important evidence for the structural and mechanistic significance of the catalytically important Pro[1] residue in 4OT.**

Electrospray ionization (ESI) mass spectrometry is fast becoming a useful tool for the study of specific noncovalent interactions involving proteins (1–5, 22). A variety of systems have already been examined, including protein–protein, protein–ligand, enzyme–substrate, and enzyme–inhibitor complexes. Most experiments carried out to date have involved the use of quadrupole mass spectrometers. However, the limited observation range of these instruments (normally $m/z < 3000$) has been a major obstacle to the detection of many noncovalent protein complexes, because charge state distributions in electrospray mass spectra are sensitive to the conformation of the analyte (6). Proteins studied by ESI under solution conditions where their native conformation is preserved generally retain only a limited number of charges, so they frequently yield ions with relatively high m/z values, >3000. To detect such ions with high m/z, an ESI source has been interfaced with a time-of-flight (TOF) mass spectrometer, which in principle has an unlimited m/z range (7). This instrument has already been used to observe noncovalent complexes with m/z as large as 16,000 (8). Here we report the application of ESI–TOF mass spectrometry to structural and mechanistic studies of the oligomeric enzyme 4-oxalocrotonate tautomerase (EC 5.3.2; 4OT).

4OT from *Pseudomonas putida mt*-2 is part of a set of inducible enzymes used by certain soil bacteria to convert aromatic hydrocarbons to intermediates in the Krebs cycle (9, 10). Specifically, the enzyme catalyzes the 1,3-allylic isomerization of 2-oxo-4-*trans*-hexenedioate to 2-oxo-3-*trans*-hexenedioate through the intermediate 2-hydroxymuconate (11). Attempts to characterize the oligomeric structure of 4OT using conventional solution phase techniques have yielded variable results. Initial characterization of 4OT using native gel electrophoresis indicated that the enzyme was a 28,000 Da protein formed by the association of eight identical subunits with an apparent molecular weight of 3,500 (10). In later studies using recombinantly derived enzyme the native molecular weight of 4OT was determined by gel permeation chromatography (M_r, 37,000 Da) and estimated by ultracentrifugation (M_r, 32,000 Da). These results suggested that 4OT was a pentamer (calculated M_r, 34,055 Da) of 62 amino acid polypeptide chains (12). However, x-ray diffraction data have since revealed that in the crystalline state the recombinant enzyme is a hexamer of identical 62 amino acid subunits (13). The subunits contain no cysteine residues and the homohexameric complex is held together by noncovalent interactions.

Recently, we established access to 4OT by total chemical synthesis; and the synthetic enzyme was used to show that the noncovalent hexamer can be readily detected by ESI–TOF mass spectrometry at m/z values between 3000 and 3500 (14). These results suggested that the 4OT hexamer is also the species present in solution. Here we report the use of ESI–TOF mass spectrometry to assess the oligomeric state of four different 4OT analogues including: (*des*Pro[1])4OT, a truncated construct in which the N-terminal proline was deleted; (Cpc[1])4OT, a derivative in which the N-terminal proline was replaced with cyclopentane carboxylate (Cpc); [Met(O)[45]]4OT, a derivative in which the side chain sulfur of Met[45] was oxidized to the sulfoxide; and (Nle[45])4OT, an analogue in which Met[45] was replaced with norleucine. Our purpose in studying [Met(O)[45]]4OT was to determine what structural effects the Met oxidation had on 4OT, because we had observed that enzyme preparations containing partially oxidized material displayed reduced enzymatic activity. The (Nle[45])4OT construct was designed to eliminate the possibility of oxidizing the enzyme during sample handling. Our goal in studying (*des*Pro[1])4OT and (Cpc[1])4OT was to further investigate the catalytic significance of the N-terminal proline, which has been implicated as the catalytic base in other studies (15).

MATERIALS AND METHODS

ESI–TOF Mass Spectrometry. Mass spectra were acquired using an ESI–TOF mass spectrometer constructed at the University of Manitoba (7). In the studies reported here, an ion acceleration voltage of 4 kV was used for TOF analysis, and ≈2 kV post acceleration was employed to improve the detection

The publication costs of this article were defrayed in part by page charge payment. This article must therefore be hereby marked "*advertisement*" in accordance with 18 U.S.C. §1734 solely to indicate this fact.

Abbreviations: ESI, electrospray ionization; TOF, time-of-flight; 4OT, 4-oxalocrotonate tautomerase; Cpc, cyclopentane carboxylate; CD, circular dichroism.

‡On leave from: Institute of Energy Problems of Chemical Physics, Chernogolovka, Moscow Region, 142432, Russia.

efficiency of the high m/z ions with low velocity, which were the object of our investigation. Samples were normally electrosprayed from a stainless steel needle (i.d., 120 μm) using flow rates of 250 nl/min; in nanoelectrospray mode (16), a small conical glass capillary (i.d., 1–3 μm) was used with flow rates of 10–25 nl/min. In either mode, mild ESI interface conditions were used ito minimize possible disruption of noncovalent complexes, i.e., low capillary (desolvation) temperature (100°C) and low declustering potential (ΔU = 80 − 120 V). Harsh interface conditions (ΔU up to 300 V) were used to perform collision-induced dissociation of complexes. The ESI interface conditions were also optimized in such a way that there was no apparent discrimination across a wide m/z range. This was made possible by introduction of a RF-quadrupole ion guide into the ESI interface (17). In this manner ions of low m/z (4OT monomer ions) and ions of high m/z (4OT hexamer ions) could be detected simultaneously with similar sensitivity.

ESI–TOF analysis was performed under both native (5 mM ammonium bicarbonate buffer, pH 7.5) and denaturing (5 mM ammonium bicarbonate buffer/0.02% formic acid, pH 4.0) conditions. ESI–TOF samples were typically prepared and analyzed at concentrations of approximately 60 μM (based on the total amount of monomer). In nanoelectrospray mode the sample concentrations used were approximately 6 μM (based on total amount of monomer).

Chemical Synthesis, Purification, and Folding of Proteins. The polypeptide chain of the 62 amino acid monomer unit of wild-type 4OT was synthesized from protected L-amino acids by highly optimized, stepwise solid-phase methods using machine-assisted *in situ* neutralization/protocols for t-butoxycarbonyl (Boc) chemistry as described (14). The polypeptide chains of (*des*Pro^1)4OT, (Nle^{45})4OT, and (Cpc^1)4OT were synthesized in the same manner. Unprotected cyclopentanecarboxylic acid (Cpc) was used instead of Boc-proline in the last coupling reaction of the (Cpc^1)4OT synthesis. The crude peptide products of the 4OT, (*des*Pro^1)4OT, (Nle^{45})4OT, and (Cpc^1)4OT syntheses were purified by reversed-phase HPLC as described (14). The [Met(O)^{45}]4OT polypeptide chain was prepared by mild oxidation of purified, synthetic 4OT: 1 mg of the 62 amino acid polypeptide chain of 4OT was dissolved in 1 ml of water containing 0.1% trifluoroacetic acid and 0.3% (vol/vol) hydrogen peroxide. Analysis of the reaction by ESI–mass spectrometry revealed that the oxidation to the sulfoxide was complete after 30 min; no sulfone was observed. The oxidized product was lyophilized and used without further purification. Analogous treatment of (Nle^{45})4OT with hydrogen peroxide had no effect on the covalent structure of this analogue (as determined by ESI–mass spectrometry), confirming that the hydrogen peroxide treatment of wild-type 4OT specifically oxidized the sulfur of Met^{45}. The synthetic 4OT proteins were each folded in assay buffer at room temperature over the course of 2 hr as previously described in the preparation of 4OT enzyme by total chemical synthesis (14)

Enzymatic Activity. The catalytic activity of each 4OT analogue in this study was assayed using the substrate 2-hydroxymuconate as described (11). Final enzyme concentrations for the 4OT, (Nle^{45})4OT, and [Met(O)^{45}]4OT assays were typically between 1 and 2 nM (based on total amount of monomer). Stock solutions of 4OT and (Nle^{45})4OT were greater than 1 μM, because losses in activity were observed in more dilute stock solutions of these enzymes. Stock solutions of [Met(O)^{45}]4OT had to be kept at concentrations greater than 40 μM to avoid significant losses in activity. Initial velocities for the enzyme catalyzed isomerization reaction were measured at six substrate concentrations ranging from 25 to 250 μM and the data were used to generate double reciprocal plots (1/v versus 1/[S]), from which V_{max}, K_m, and k_{cat} values were extracted. No catalytic activity was detected for (Cpc^1)4OT and [Met(O)^{45}]4OT even in assays performed at enzyme concentrations as high as 10 μM. Enzyme concentrations were initially established by amino acid analysis after acid hydrolysis and routinely determined from HPLC peak areas.

Circular Dichroism (CD) Spectroscopy. CD spectra of 4OT and analogues were measured in 50 mM sodium borate buffer (pH 7.0), at concentrations of approximately 10 μM using an AVIV 60 DS instrument. CD spectra for these protein samples were recorded from 190 to 260 nm at 20°C using a 3.0-ml quartz cuvette with a 1-cm path length. The results are presented as a plot of mean molar ellipticity per residue ([θ], deg·cm^2 dmol^{-1}) versus wavelength in 0.5 nm increments. The helical content of each analogue was estimated from the magnitude of its molar ellipticity value, [θ], at 222 nm (18).

RESULTS AND DISCUSSION

ESI–TOF Analysis of 4OT. ESI–TOF mass spectra of 4OT recorded under native and denaturing solution conditions are shown in Fig. 1. The most intense signals in the spectrum acquired under native electrospray conditions (5 mM ammonium bicarbonate buffer, pH 7.5) were those of the multiply-charged monomer and hexamer (Fig. 1*A*). Only weak signals representative of the dimer and pentamer were observed. The amount of pentamer observed was strongly dependent on the declustering (capillary-skimmer) potential (see Fig. 3), indicating that it arises from decomposition of the hexamer in the latter stages of the electrospray process. Analysis of 4OT under denaturing conditions (5 mM ammonium bicarbonate buffer/0.02% formic acid, pH 4.0) yielded only multiply-charged ions of the monomer and traces of dimer with no detectable hexamer (Fig. 1*B*). The relatively small amount of dimer is consistent with nonspecific associations often observed in the ESI analysis of samples at high (60 μM) concentration. The absence of multiply-charged hexamer ions in the spectrum recorded under denaturing solution conditions (Fig. 1*B*) helps confirm the specific, noncovalent nature of the hexamer complex that was the major species detected under native

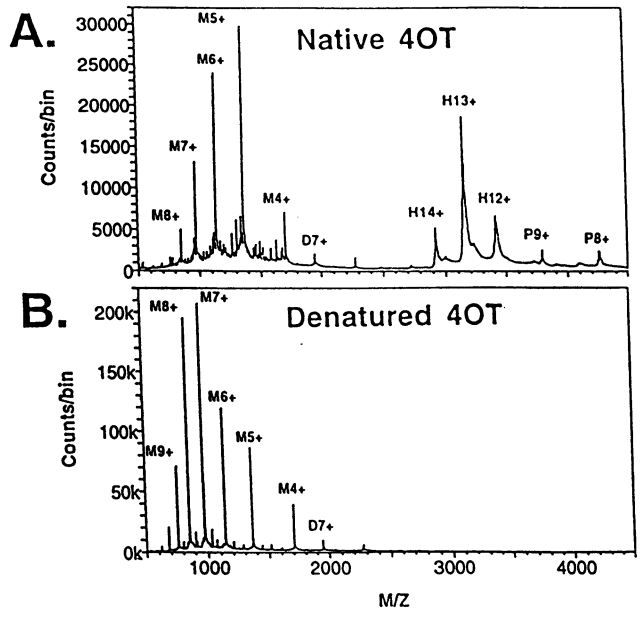

FIG. 1. ESI–TOF mass spectra of 4OT. (*A*) The major signals observed in the mass spectra acquired under native solution conditions (5 mM ammonium bicarbonate buffer, pH 7.5, ΔU = 120 V) are due to multiply-charged signals of the hexamer (H) and monomer (M). (*B*) Under denaturing solution conditions (5 mM ammonium bicarbonate buffer, 0.02% formic acid, pH 4.0, ΔU = 120 V) multiply-charged monomer ions are the only major species detected. Minor peaks due to multiply-charged dimer (D) and pentamer (P) ions are also labeled in each spectra.

electrospray conditions (Fig. 1*A*). Furthermore, the native mass spectrum provides evidence that the hexamer signal results from structurally specific complexation and not random aggregation of the monomer, because of the appearance of only weak signals for the dimer and pentamer along with the absence of multiply-charged trimer and tetramer ions.

A more detailed analysis of the native and denatured mass spectra of 4OT (Fig. 1) is shown in Fig. 2. The results obtained after summing the multiply-charged hexamer signals (Fig. 2*A*) revealed that the mass of the major peak (40,861 ± 4 Da) in this deconvolution was in good agreement with that expected for the hexameric complex 4OT (calculated mass, 40,863 Da). The "tailing" of the peak toward high mass is consistent with the formation of multiple salt adducts, such as those with CF_3COO^- and various cations such as Na^+ and K^+. A discrete, smaller peak at 40,761 ± 4 Da is also discernible and may be due to the formation of complexes containing truncated polypeptide chains present as impurities in the sample. A similar analysis of the monomer species observed in the native and denatured spectra (Fig. 2 *B* and *C*) showed a greater abundance of lower molecular weight impurity peaks, relative to the full-length monomer peak (6811 Da), in the spectrum of native 4OT. This can be attributed to discrimination against these truncated monomers in the folding process to form the hexamer, as full-length monomers are more likely to be consumed during complex formation.

The relative ion intensities of the monomer and hexamer peaks in the native mass spectrum (shown in Fig. 1*A*) were typical of those observed in spectra collected under normal electrospray conditions. However, the significance of the observed ion yields is difficult to evaluate as it is also not clear if the monomers were initially present in the sample solution or if they resulted from decomposition of the hexamer during the ESI process. In an effort to reduce possible dissociation of the hexamer during the electrospray process we also analyzed 4OT by nanoelectrospray, which was expected to be milder than our normal electrospray conditions (16). The native ESI–TOF mass spectrum of 4OT acquired by nanoelectrospray is shown in Fig. 3*A*. Under these conditions the hexamer was the only species observed, suggesting that the sample was nearly all hexamer in solution prior to ESI. The hexamer signals in Fig. 3*A* are broader than those in Fig. 1*A*, presumably due to salt adduction and/or incomplete desolvation of the complex. These adducts are not detected at higher declustering potentials (see below).

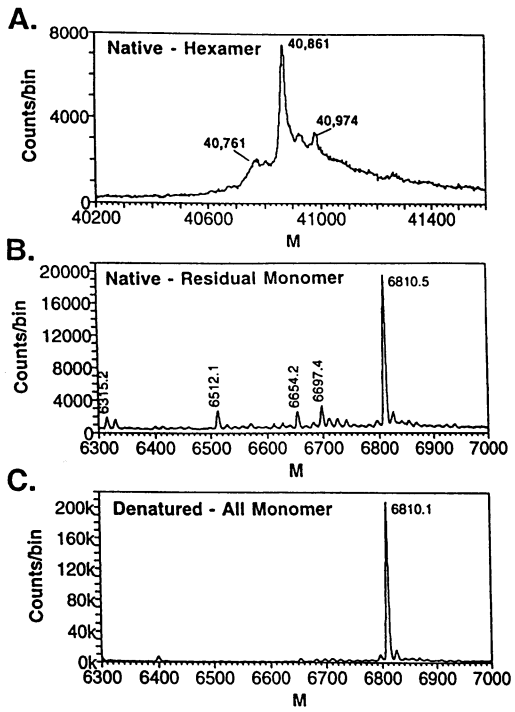

FIG. 2. Analysis of the multiply-charged ion signals in Fig. 1. (*A*) Summation of the multiply-charged hexamer signals in the native mass spectrum shown in Fig. 1*A*. (*B*) Summation of the residual monomer ion signals in the native mass spectrum shown in Fig. 1*A*. (*C*) Summation of the monomer ion signals in the denatured mass spectrum shown in Fig. 1*B*.

The 4OT hexamer complex detected under native, nanoelectrospray conditions was readily dissociated by increasing the declustering potential as shown in Fig. 3. Raising the declustering potential increases the collisional energy of molecules at the electrospray interface resulting in the disruption of noncovalent bonds. The dissociation data in Fig. 3 show that decomposition of the hexamer results in the loss of monomeric species. These results do not appear to be consistent with the crystallographic structure in which the hexamer complex resembles a trimer of dimers.

The fragmentation patterns observed for the hexamer under normal electrospray conditions (results not shown) were similar to those shown in Fig. 3. However, it should be noted that under normal electrospray conditions it was not possible to record spectra containing *only* hexameric species even at declustering potentials as low as 40 V. ESI–TOF analysis of 4OT under normal electrospray conditions using low declustering potentials (40–120 V) consistently yielded spectra containing small but significant amounts of monomer along with intact hexamer. The absence of monomers in the ESI–TOF analysis of 4OT under nanoelectrospray conditions suggests that their presence under normal electrospray conditions results from decomposition of the hexamer during the ESI process.

ESI–TOF Analysis of 4OT Analogues. ESI–TOF mass spectrometry was used to establish the oligomeric state of each 4OT analogue. The mass spectra are shown in Fig. 4 (a typical spectrum of wild-type 4OT is also included for comparison). The spectra in Fig. 4 were acquired under identical normal electrospray conditions using the same buffer (5 mM ammonium bicarbonate, pH 7.5), needle position, and declustering potential (ΔU = 120 V). The results obtained with (Nle^{45})4OT and (Cpc^1)4OT were similar to those obtained with 4OT (Fig.

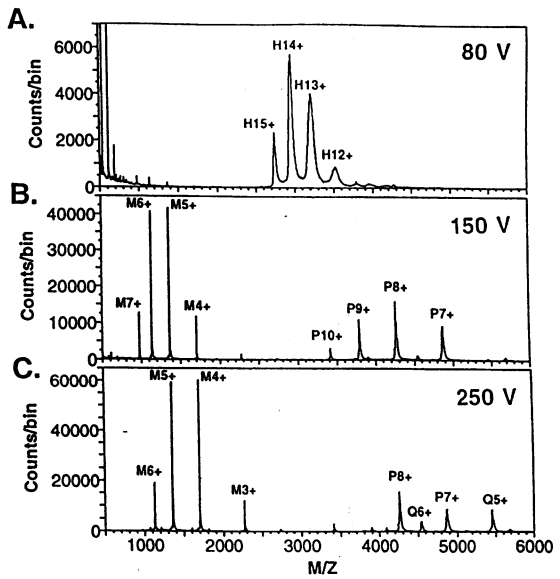

FIG. 3. Nanoelectrospray results with 4OT. (*A*) Using a declustering potential of 80 V only multiply-charged hexamer (H) ions are detected. The hexamer is readily dissociated to pentamer (P), tetramer (T), and monomer (M) species at declustering potentials of 150 V (*B*) and 250 V (*C*).

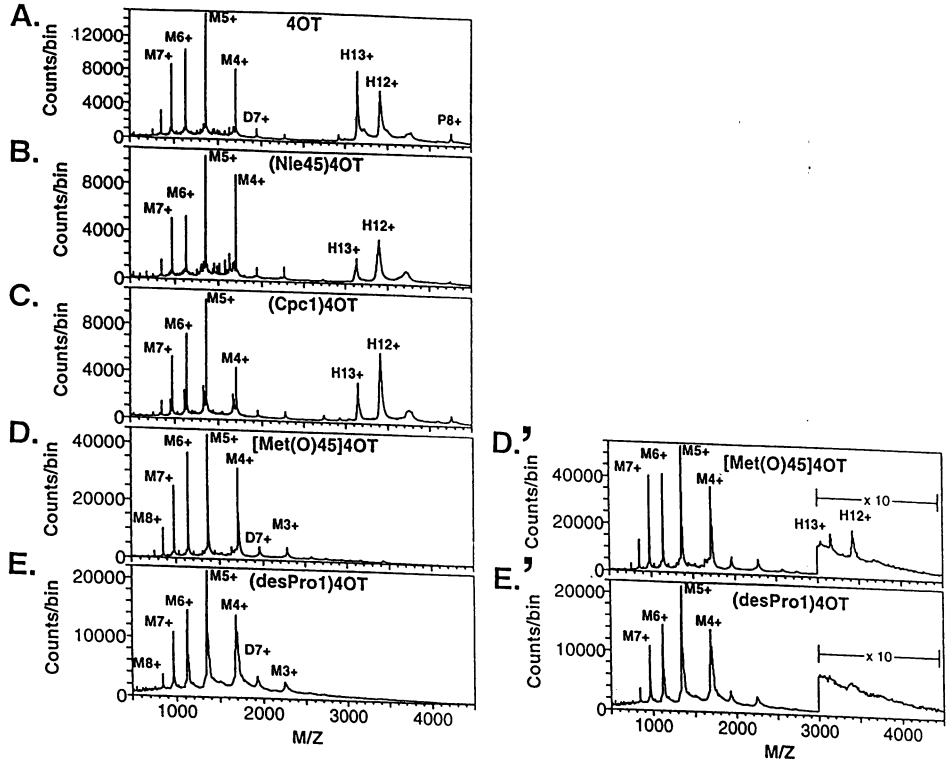

FIG. 4. ESI–TOF analysis of 4OT analogues. The native mass spectra (acquired under identical conditions: 5 mM ammonium bicarbonate buffer, pH 7.5, ΔU = 120 V) are shown for each analogue: (*A*) 4OT, (*B*) (Nle^{45})4OT, (*C*) (Cpc^{1})4OT, (*D*) [Met(O)^{45}]4OT, and (*E*) (*des*Pro^{1})4OT. The native mass spectra of [Met(O)^{45}]4OT and (*des*Pro^{1})4OT are also shown with a 10-fold vertical scale expansion in the high *m/z* region (*D'* and *E'*, respectively). Strong hexamer signals were detected for 4OT, (Nle^{45})4OT, and (Cpc^{1})4OT. Only very weak signals for the [Met(O)^{45}]4OT hexamer were observed, and there was no detectable hexamer in the (*des*Pro^{1})4OT sample.

4 *A–C*). In each case, intense signals for the +12 and +13 charge states of hexamer species were observed. However, notably different results were obtained with [Met(O)^{45}]4OT and (*des*Pro^{1})4OT. Analysis of these samples under the native ESI conditions yielded predominantly multiply-charged monomer ions (Fig. 4 *D* and *E*). A 10-fold vertical scale expansion of the high mass region in the [Met(O)^{45}]4OT spectra revealed only very weak signals corresponding to the +12 and +13 charge state of the [Met(O)^{45}]4OT hexamer (Fig. 4*D'*). Using a similar scale expansion, there was still no detectable hexamer (detection limit: < ≈0.5%) in the (*des*Pro^{1})4OT sample (Fig. 4*E'*).

The amounts of hexamer and monomer observed in the native mass spectra of 4OT, (Nle^{45})4OT, and (Cpc^{1})4OT were approximately the same, and the ratio of hexamer to monomer in each case was 2.8, 2.3, and 3.4, respectively (as calculated from peak areas summed over the multiple charge states of each species). A much smaller value of 0.06 was obtained from the mass spectrum of [Met(O)^{45}]4OT shown in Fig. 4*D'*. The absence of multimeric species in the native mass spectrum of the (*des*Pro^{1})4OT analogue allowed us to confirm that there was no discrimination in detection efficiencies for the monomer and hexamer and to estimate the relative amount of hexamerization observed in the native mass spectrum of 4OT. This was accomplished by analyzing a defined mixture of 4OT and (*des*Pro^{1})4OT under both native (pH 7.5) and denaturing (2% acetic acid, pH 2) conditions (results not shown) and then comparing the relative signal intensities of the 4OT and (*des*Pro^{1})4OT monomer species (i.e., peak areas summed over all monomeric charge states) in each case. Under denaturing conditions the ratio of 4OT monomer to (*des*Pro^{1})4OT monomer was 2.7 and remained relatively constant during ESI at declustering potentials (ΔU) of 60 to 300 V. Under native conditions it varied from 0.6 to 2.0 as ΔU was changed from 60 to 300 V. Thus, under the normal, native electrospray conditions with ΔU = 60 V, the ratio of 4OT monomer to (*des*Pro^{1})4OT monomer was only ≈20% of that measured under denaturing conditions, indicating that ≈80% of the 4OT polypeptide chains were present as multimers (predominantly folded hexamer) at this low declustering potential. At ΔU = 300 V the ratio of 4OT monomer to (*des*Pro^{1})4OT monomer was ≈80% of that measured under denaturing conditions, indicating that ≈20% of the 4OT polypeptide chains were still detected as multimers, even at this high declustering potential.

Our ESI–TOF results with 4OT, (Nle^{45})4OT, and (Cpc^{1})4OT (Fig. 4 *A–C*) indicate that the 62 residue polypeptide chains of 4OT, (Nle^{45})4OT, and (Cpc^{1})4OT each folded in solution to form a hexameric enzyme complex. The absence of any multimeric species in the native mass spectrum of (*des*Pro^{1})4OT (Fig. 4 *E'*) shows that this truncated analog has no discernible quaternary structure, suggesting that it does not fold correctly. The presence (albeit weak) of multiply-charged hexamer ions in the native mass spectrum of [Met(O)^{45}]4OT indicates that this construct is capable of forming a homohexameric complex (Fig. 4 *D'*). However, the ratio of hexamer to monomer in the [Met(O)^{45}]4OT spectrum was significantly smaller (≈50-fold less) than the hexamer to monomer ratio in the 4OT, (Nle^{45})4OT, and (Cpc^{1})4OT spectra. Analysis of [Met(O)^{45}]4OT under milder nanoelectrospray conditions also yielded spectra with relatively small hexamer to monomer ratios (data not shown). These results suggest that the [Met(O)^{45}]4OT hexamer is defined by significantly weaker protein–protein interactions and is thus more easily dissociated during the ESI process.

CD. Additional structural studies on 4OT and the analogues were performed using CD spectroscopy. CD spectra were recorded in 50 mM sodium borate buffer (pH 7.0), at 25°C, and the results are shown in Fig. 5. The percent helicities calculated

for 4OT, (Nle[45])4OT, [Met(O)[45]]4OT, and (Cpc[1])4OT were each approximately 26% and were in relatively good agreement with that previously reported for recombinant 4OT (21%) (19). Furthermore, the UV–CD spectra recorded for 4OT, (Nle[45])4OT, and (Cpc[1])4OT were essentially identical. These results provide evidence that the secondary structural features of the (Nle[45])4OT and (Cpc[1])4OT analogues are similar to those of the wild-type enzyme. In contrast, the unique minimum at 208 nm observed in the UV–CD spectrum of [Met(O)[45]]4OT suggests that the secondary structure of this analogue may be slightly altered from that of 4OT, (Nle[45])4OT, and (Cpc[1])4OT. The essentially featureless spectrum of the (*des*Pro[1])4OT analogue showed that this polypeptide has very little defined secondary structure.

Enzymatic Activity. The catalytic efficiency of each 4OT analogue was determined by studying the kinetics of the conversion of 2-hydroxymuconate to 2-oxo-3-*trans*-hexenedioate. The K_m, k_{cat}, and k_{cat}/K_m values determined for 4OT and each analogue are reported in Table 1. These kinetic parameters were measured using standard assay conditions for 4OT (20 mM sodium phosphate buffer, pH 7.4). Unfortunately, accurate K_m and k_{cat} values could not be determined under the exact solution conditions used for native ESI–TOF analysis (5 mM ammonium bicarbonate buffer, pH 7.5) because concentrations of the dicarboxylic acid substrate greater than 100 μM exceeded the buffering capacity of the ammonium bicarbonate buffer. However, at low substrate concentrations (<100 μM) the initial velocities measured for the 4OT-catalyzed reaction in 20 mM sodium phosphate buffer (pH 7.4) were comparable to those measured in 5 mM ammonium bicarbonate buffer (pH 7.5) indicating that the enzyme is fully active under the solution conditions used in our native ESI–TOF experiments.

The kinetic results in Table 1 show that the (Nle[45])4OT and [Met(O)[45]]4OT analogues displayed enzymatic activity comparable to that of 4OT. The small increase in K_m for [Met(O)[45]]4OT suggests that oxidation of Met[45] may slightly decrease the ability of 4OT to bind its substrate. Kinetic parameters are not reported for (Cpc[1])4OT and (*des*Pro[1])4OT in Table 1 because no rate enhancement over the nonenzymatic chemical ketonization of 2-hydroxymuconate to 2-oxo-3-*trans*-hexenedioate (uncatalyzed rate: 8.7×10^{-4} s^{-1}) was detected (detection limit: $k_{cat} \approx 1$ s^{-1}) for these analogues (7). It is also important to note that the full enzymatic activity of [Met(O)[45]]4OT reported in Table 1 was only obtained when enzyme stock solutions greater than 40 μM (based on monomer) in concentration were used. In contrast, stock solutions of 4OT and (Nle[45])4OT as dilute as 1 μM (based on monomer) gave full enzymatic activity. Enzyme stock solutions of 4OT, (Nle[45])4OT, and [Met(O)[45]]4OT below these critical concentrations lost their enzymatic activity over a period of several hours, suggesting that the active enzyme complex was slowly dissociated in these dilute solutions.

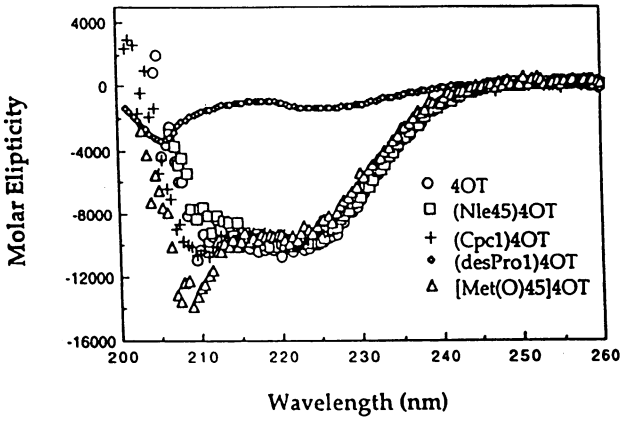

FIG. 5. Far CD spectra for 4OT, (Nle[45])4OT, (Cpc[1])4OT, [Met(O)[45]]4OT, and (*des*Pro[1])4OT.

Table 1. Kinetic parameters for synthetic 4OT and analogues

Analogue	K_m,* μM	k_{cat},* s^{-1} $\times 10^{-3}$	k_{cat}/K_m,* M^{-1}·s^{-1} $\times 10^{-7}$
4OT	90 ± 20	2.9 ± 0.53	3.2 ± 1.3
[Met(O)[45]]4OT	290 ± 100	3.0 ± 1.04	1.0 ± 0.7
(Nle[45])4OT	50 ± 10	2.4 ± 0.20	4.6 ± 1.3
(Cpc[1])4OT		Not active†	
(*des*Pro[1])4OT		Not active†	

*, ± one SD.
†Detection limit: $k_{cat} \approx 1$ s^{-1}.

These observations and the dramatically different oligomerization properties found for 4OT, (Nle[45])4OT, and [Met(O)[45]]4OT in our native ESI–TOF experiments prompted us to study the kinetic behavior of these analogues more closely. Therefore, we measured initial velocities of the 4OT-, (Nle[45])4OT-, and [Met(O)[45]]4OT-catalyzed reaction at identical enzyme and substrate concentrations but using enzyme diluted into assay buffer (immediately before assay) from stock solutions ranging in concentration from 0.01 to 60 μM. The apparent dissociation constants (K_D) for 4OT, (Nle[45])4OT, and [Met(O)[45]]4OT were estimated from these data, based on the enzyme stock solution concentration at which each analogue displayed 50% of its maximal activity (Fig. 6). The K_D of 4OT was estimated at 0.04 μM and was increased approximately 10- and 1000-fold for (Nle[45])4OT and [Met(O)[45]]4OT, respectively.

Structural and Mechanistic Implications. The ESI–TOF results along with the CD and kinetic data for the 4OT analogues have increased our knowledge of the structure and function of this highly efficient enzyme. The characterization of [Met(O)[45]]4OT has enabled us to understand the effects of oxidation of the methionine side chain on the structure and function of 4OT. The kinetic data and ESI–TOF analysis of [Met(O)[45]]4OT showed that this mutant folds to form a fully active hexameric enzyme complex resembling that of 4OT. However, the apparent dissociation constants suggest that the noncovalent interactions defining the hexameric, [Met(O)[45]]4OT complex are weaker than those in 4OT. The ESI–TOF results also support this finding.

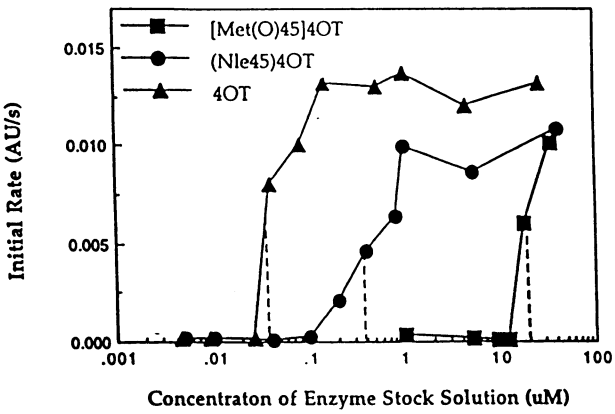

FIG. 6. Initial velocities for the 4OT-, (Nle[45])4OT-, and [Met(O)[45]]4OT-catalyzed reactions at identical enzyme and substrate concentrations but using enzyme diluted into assay buffer (immediately before assay) from stock solutions ranging in concentration from 0.01 to 60 μM. Based on the enzyme stock solution concentration at which each analogue displayed 50% of its maximal activity, the apparent dissociation constants (K_D) for 4OT, (Nle[45])4OT, and [Met(O)[45]]4OT are approximately 0.04, 0.3, and 20 μM, respectively.

The physical and kinetic characterization of (Cpc^1)4OT and (*des*Pro^1)4OT reported here also provided direct evidence for the functional significance of the N-terminal residue (Pro^1) in 4OT. ESI–TOF analysis of the (*des*Pro^1)4OT construct under native solution conditions indicated that this truncated 4OT mutant did not form multimeric (hexamer) complexes. The featureless UV–CD spectrum recorded for (*des*Pro^1)4OT also showed that this polypeptide has very little secondary structure. These results suggest that Pro^1 is essential for maintaining higher order structure in 4OT. Furthermore, studies with (Cpc^1)4OT permitted direct evaluation of the mechanistic role of Pro^1 in 4OT catalysis.

Replacement of the ring nitrogen of Pro^1 by a methylene group in (Cpc^1)4OT made it possible to delete this secondary amine functionality in 4OT and still maintain the structural integrity of the enzyme complex as shown by ESI–TOF mass spectrometry and UV–CD spectroscopy. The complete lack of detectable activity (detection limit $\approx 1\ s^{-1}$) in the (Cpc^1)4OT analogue provides direct evidence that the secondary amine functionality of the N-terminal proline plays a critical role in the 4OT-catalyzed isomerization reaction. These conclusions about the catalytic significance of the N-terminal proline are also consistent with those drawn from earlier x-ray crystallographic data on a 4OT isozyme and from inhibition studies with an active-site-directed irreversible inhibitor of 4OT (20, 21). Pro^1 was also implicated as the catalytic base in both of these studies.

Significance. The 4OT analogues characterized in this study contained very subtle differences in their covalent structure: (*des*Pro^1)4OT had only a single amino acid deleted; and (Nle^{45})4OT, [Met(O)^{45}]4OT, and (Cpc^1)4OT each differ from wild-type 4OT by only a single atom. Despite these small changes, however, there were clear differences in the ESI–TOF spectra: intense hexamer signals were detected for 4OT, (Nle^{45})4OT, and (Cpc^1)4OT, but *not* for (*des*Pro^1)4OT or [Met(O)^{45}]4OT. The correlation of these results with other physical and kinetic measurements provides strong evidence for the relevance of the protein–protein complexes detected in our ESI–TOF experiments to the solution phase behavior of this enzyme molecule. We conclude, therefore, that ESI–TOF can be a very sensitive technique for examining the effects that subtle differences in primary structure can have on an enzyme's higher order structure.

This work was supported by funds from the National Institutes of Health (S.B.H.K., C.P.W., and K.G.S.) and the National Science and Engineering Research Council of Canada (K.G.S. and I.C.). M.C.F. was the recipient of a National Research Service Award sponsored by the National Institutes of Health.

1. Light-Wahl, K. J., Schwartz, B. L. & Smith, R. D. (1994) *J. Am. Chem. Soc.* 116, 5271–5273.
2. Loo, J. (1995) *J. Mass Spectrom.*, 180–183.
3. Eckart, K. & Spiess, J. (1995) *J. Am. Soc. Mass Spectrom.* **6,** 912–919.
4. Shwartz, B. L., Bruce, J. E., Anderson, G. A., Hoffstadler, S. A., Rockwood, A. L., Smith, R. D., Chilkoti, A. & Stayton, P. S. (1995) *J. Am. Soc. Mass Spectrom.* **6,** 459–465.
5. Baca, M. & Kent, S. B. H. (1992) *J. Am. Chem. Soc.* **114,** 3992.
6. Chowdhury, S. K., Katta, V. & Chait, B. T. (1990) *J. Am. Chem. Soc.* **112,** 9012–9013.
7. Verentchikov, A. N., Ens, W. & Standing, K. G. (1994) *Anal. Chem.* **66,** 126–133.
8. Chernushevich, I. V., Ens, W., Standing, K. G., Loewen, P. C., Fitzgerald, M. C., Kent, S. B. H., Werlen, R. C., Lankinen, M., Tang, X.-J., Brewer, C. F. & Saha, S. (1995) *Proceedings of the 43rd Annual Conference on Mass Spectrometry and Allied Topics,* Atlanta, GA (ASMS, Santa Fe, NM), p. 1327.
9. Harayama, S., Lehrbach, P. R. & Timmis, K. (1984) *J. Bacteriol.* **160,** 251–255.
10. Harayama, S., Rekik, M., Ngai, K. L. & Ornston, L. N. (1989) *J. Bacteriol.* **171,** 6251–6258.
11. Whitman, C. P., Aird, B. A., Gillespie, W. R. & Stolowich, N. J. (1991) *J. Am. Chem. Soc.* **113,** 3154–3162.
12. Chen, L. H., Kenyon, G. L., Curtin, F., Harayama, S., Bembenek, M. E., Hajipour, G. & Whitman, C. P. (1992) *J. Biol. Chem.* **267,** 17716–17721.
13. Roper, D. I., Subramanya, H. S., Shingler, V. & Wigley, D. B. (1994) *J. Mol. Biol.* **243,** 799–801.
14. Fitzgerald, M. C., Chernushevich, I., Standing, K. G., Kent, S. B. H. & Whitman, C. P. (1995) *J. Am. Chem. Soc.* **117,** 11075-11080.
15. Subramanya, H. S., Roper, D. I., Dauter, Z., Dodson, E. J., Davies, G. J., Wilson, K. S. & Wigley, D. B. (1996) *Biochemistry* **35,** 792–802.
16. Wilm, M. S. & Mann, M. (1994) *Int. J. Mass Spectrom. Ion Phys.* **136,** 167–180.
17. Krutchinsky, A. N., Chernushevich, I. V., Spicer, V., Ens, W. & Standing, K. G. (1995) *Proceedings of the 43rd Annual Conference on Mass Spectrometry and Allied Topics*, Atlanta, GA (ASMS, Santa Fe, NM), p. 126.
18. Chen, Y. H., Yang, J. T. & Chau, K. H. (1974) *Biochemistry* **13,** 3350–3359.
19. Stivers, J. T., Whitman, C. P. & Mildvan, A. S. (1994) *Am. Chem. Soc. Abstr.* **208,** 261.
20. Stivers, J. T., Abeygunawardana, C., Mildvan, A. S., Hajipour, G., Whitman, C. P. & Chen, L. H. (1996) *Biochemistry* **35,** 803–813.
21. Stivers, J. T., Abeygunawardana, C., Mildvan, A. S., Hajipour, G. & Whitman, C. P. (1996) *Biochemistry* **35,** 814–823.
22. Tang, X.-J., Brewer, F. C., Saha, S., Chernushevich, I., Ens, W. & Standing, K. G. (1994) *Rapid Commun. Mass Spectrom.* **8,** 750–754.